

## Supporting Information for

# Record-Efficiency Flexible Perovskite Solar Cell and Module Enabled by a Porous-Planar Structure as an Electron Transport Layer

Jaehoon Chung<sup>1,=</sup>, Seong Sik Shin<sup>1,=</sup>, Kyeongil Hwang<sup>1</sup>, Geunjin Kim<sup>1</sup>, Ki Woong Kim<sup>1</sup>, Da  
Seul Lee<sup>1</sup>, Wansun Kim<sup>2</sup>, Boo Soo Ma<sup>2</sup>, Young-Ki Kim<sup>3</sup>, Taek-Soo Kim<sup>2</sup>, and Jangwon Seo<sup>1,\*</sup>

### Affiliations:

<sup>1</sup>Division of Advanced Materials, Korea Research Institute of Chemical Technology,  
141 Gajeong-Ro, Yuseong-Gu, Daejeon 305-600, Korea

<sup>2</sup>Department of Mechanical Engineering, Korea Advanced Institute of Science and  
Technology (KAIST), 291, Daehak-ro, Yuseong-Gu, Daejeon 34141, Korea

<sup>3</sup>Center Research Facilities, Ulsan National Institute of Science and Technology  
(UNIST), 50 UNIST-gil, Eonyang-eup, Ulju-gun, Ulsan 44919, Republic of Korea

\*Correspondence. Email: [jwseo@kriict.re.kr](mailto:jwseo@kriict.re.kr)

=These authors contributed equally: Jaehoon Chung; Seong Sik Shin

## **METHODS**

### Synthesis of $Zn_2SnO_4$ nanoparticles

All chemicals for the preparation of NPs were of reagent grade and were used without further purification.  $ZnCl_2$  (12.8 mmol, Aldrich) and  $SnCl_4 \cdot 5H_2O$  (6.4 mmol, Aldrich) were dissolved in deionized water (80 ml) under vigorous magnetic stirring.  $N_2H_4 \cdot H_2O$  8ml was then added dropwise to the reaction solution. White precipitates formed immediately, and this solution, including the precipitate, was heated in an autoclave reactor at 180 °C for 12 h. The obtained products were thoroughly washed with deionized water and ethanol and were then dispersed in isopropyl alcohol, resulting in a colloidal solution.

### Fabrication of unit cell on glass and flexible substrate

The  $SnO_2$  precursor solution was obtained from  $SnO_2$  colloidal precursor (Tin(IV) oxide, 15% in  $H_2O$  colloidal disperse, Alfa Aesar) diluted in water with volumetric ratio 1:5. For  $SnO_2$  planar structured perovskite solar cells (PSCs), a 30 nm of nanoparticle (np)- $SnO_2$  film was deposited by spin-coating for 50 s at 4000 rpm onto the In-doped  $SnO_2$  (ITO,  $8\Omega/\square$ ) substrate using the  $SnO_2$  precursor solution, and then heat treated on a hot plate in ambient air at 150 °C for 1 hour. For the  $Zn_2SnO_4$  (ZSO) porous planar structured PSCs, 100 nm of ZSO nanoparticles were sequentially deposited by spin-coating for 50 s at 3000 rpm onto np- $SnO_2$ /ITO/glass substrate, and then heat treated on a hot plate in ambient air at 150 °C 1 hour. For flexible device fabrication, np- $SnO_2$  and porous-ZSO ETL were deposited onto PEN/ITO ( $15\Omega/\square$ , 87.5% of transmittance, Nano Clean Tech) substrate by using the same deposition procedure onto glass substrate, and then heat treated on hot plate at 100 °C for 1 hour. To deposit perovskite absorbing layer,  $(FAPbI_3)_{0.95}(MAPbBr_3)_{0.05}$ , the perovskite precursor solution was prepared by dissolving 1.26 mmol of  $PbI_2$  (Alfa Aesar), 1.26 mmol of FAI (dyesol), 0.06 mmol of  $MAPbBr_3$  and 0.5 mmol of  $MACl$  (Sigma Aldrich) in DMF/DMSO (8:1 v/v) mixed solvent. Then, the solution were then coated onto the np- $SnO_2$ /ITO and np-

SnO<sub>2</sub>/porous-ZSO/ITO substrate by two consecutive spin-coating steps, at 1000 and 5000 rpm for 3 s and 15 s, respectively. During the second spin-coating step, 1 mL ethyl ether was poured onto the substrate. Then, the resultant substrate was heated on a hot plate at 100 °C for 1 hour. For deposition of hole-transport materials, a Spiro-OMeTAD (LUMTEC)/chlorobenzene (91 mg/ 1 ml) solution with an additive of 21 µl of Li-bis(trifluoromethanesulfonyl) imide (Li-TFSI)/acetonitrile (540 mg/ 1 ml), 35 µl of 4-tert-butylpyridine (TBP) and 9 µl of tris(2-(1H-pyrazol-1-yl)-4-tert-butylpyridine)-cobalt(III) tris(bis(trifluoromethylsulfonyl)imide (FK 209)/acetonitrile (376 mg/1 ml) was spin-coated on (FAPbI<sub>3</sub>)<sub>0.95</sub>(MAPbBr<sub>3</sub>)<sub>0.05</sub>/np-SnO<sub>2</sub>/ITO and (FAPbI<sub>3</sub>)<sub>0.95</sub>(MAPbBr<sub>3</sub>)<sub>0.05</sub>/porous-ZSO/np-SnO<sub>2</sub>/ITO substrate at 2000 rpm for 30 s. Finally, Au counter electrode was deposited by thermal evaporation. The entire unit cell size is 25 mm x 25 mm. Four active areas with size of 4 mm x 4 mm were fabricated on the unit cell by superposing ITO and Au electrodes. Photovoltaic performance was measured by masking on the active area with a metal mask (0.0935 cm<sup>2</sup>). In particular, surface treatment on perovskite layer has conducted for Newport certification samples.<sup>1</sup>

#### Fabrication of 100 cm<sup>2</sup> and 225 cm<sup>2</sup> flexible perovskite solar mini modules

The module composed of 15-stripes and 22-stripes connected in series was fabricated using a pulsed-type UV laser scribe (Nd:YVO<sub>4</sub> 355 nm with 2 W, 80 khz, Spectra Physics). For fabrication of flexible solar modules, 12 cm × 12 and 17 cm x 17 cm (1 cm of margin on both side edge for encapsulation) PEN/ITO substrate was patterned by the laser with a power of 0.7 W, a frequency of 70 kHz and a spot size of 35 µm and a scribing width of 150 µm (P1). Next, all layers including np-SnO<sub>2</sub>/porous-ZSO/perovskite/Spiro-OMeTAD were scribed together by the laser with a power of 0.6 W, a frequency of 70 kHz, and a spot size of 35 µm and a scribing width of 100 µm (P2). Finally, after thermal evaporation of Au, the top electrode was patterned by the laser with a power of 0.35 W, a frequency of 70 kHz, and a spot size of 35 µm and a scribing width of 150 µm (P3). The modules were designed to have a geometric

fill factor of 90%. Planar SnO<sub>2</sub> layer was deposited on the P1-pattered ITO/PEN substrate by low angle-blade coating (solution-shearing) method (PMC-300, Pems-Korea). A SnO<sub>2</sub> colloidal precursor (Tin(IV) oxide, 15% in H<sub>2</sub>O colloidal disperse, Alfa Aesar) was used for coating, and 150 µl of SnO<sub>2</sub> solution was loaded in the gap (around 150 µm) between the blade and the substrate and blade angle was adjusted to 7°. The blade coating speed of solution shearing was 1 mm s<sup>-1</sup> and precursor solution was coated on the substrate through the meniscus which formed by blade coating. After coating process, thermal annealing process at 100 °C for 30 min was followed. For porous Zn<sub>2</sub>SnO<sub>4</sub> layer, the same Zn<sub>2</sub>SnO<sub>4</sub> solution with unit-cell was used for solution-shearing onto the SnO<sub>2</sub> layer. A 200 µl of Zn<sub>2</sub>SnO<sub>4</sub> solution was loaded in the coating gap, and the coating speed was fixed to 1 mm s<sup>-1</sup>. The Zn<sub>2</sub>SnO<sub>4</sub> solution-shearing process was repeated several times to obtain a fully covered porous Zn<sub>2</sub>SnO<sub>4</sub> layer with desired film-thickness for preventing shunt recombination throughout the large area over 100 cm<sup>2</sup>. The Zn<sub>2</sub>SnO<sub>4</sub> was also thermally annealed at 100 °C for 60 min after consecutive coatings. Then, for fabrication of the perovskite layer, 1 ml of the same perovskite solution with unit cell was loaded onto the PEN/ITO/np-SnO<sub>2</sub>/porous-ZSO substrate and deposited by two consecutive spin-coating steps of 1000 rpm and 3000 rpm for 5 s and 15 s, respectively. During the second spin-coating step (3000 rpm), 10 ml of diethyl ether was poured onto the substrate. The intermediate phase film was put on a hotplate at 100 °C for 60 min. For Spiro-OMeTAD deposition onto the perovskite, 1 ml of the same Spiro-OMeTAD solution with unit-cell was spin-coated onto the perovskite layer at 2000 rpm for 30 s. All the module-fabrication processes were carried out in air with the controlled temperature and relative humidity around 25 °C and 25 %, respectively. Finally, Au electrode was thermally evaporated at vacuum condition. In particular, surface treatment on perovskite layer has conducted to obtain best PCE of sub module.<sup>1</sup>

## Characterization

The morphologies and microstructures were investigated by field emission scanning electron microscopy (FE-SEM, Mira 3 LMU FEG, Tescan) and transmission electron microscopy (TEM, Titan G2). High resolution X-ray diffraction (HR-XRD, SmartLab, Rigaku) was conducted to analyze crystallinity of each perovskite layer from 5 to 50 degree. X-ray photoelectron spectroscopy (XPS) studies were carried out using a Thermo VG Scientific K-Alpha. Ultraviolet photoelectron spectroscopy (UPS) equipped with XPS (He I: 21.2 eV, Kratos, AXIS-Nova Ultra DLD) was used for the analysis of the work function and band structure of SnO<sub>2</sub> and ZSO. Space-charge limited current of the samples (ITO/electron transport layer (ETL)/perovskite/ [6,6]-phenyl-C61-butyric acid methyl ester/Au) were measured with electrochemical measurement system (PGSTAT30, AutoLab, EcoChemie) at various voltages. Using the sample of ITO/ETL/perovskite/Spiro-OMeTAD/Au, Mott-Schottky (M-S) plots were deduced from capacitance-voltage measurements in the voltage range 0 to 1.3 V with a 10 mV AC signal (1kHz) under dark conditions (PGSTAT30, AutoLab, EcoChemie). Atomic force microscopy (AFM) was measured by using Nanoscope IV (Veeco Instrument, Inc) with Pt tip (Bruker) in tapping mode. Time-resolved photoluminescence (TRPL) decay profiles were obtained with the 532 nm excitation (pulse energy attenuated to ~1 μJ) of an optical parametric oscillator (OPO) laser system (NT 342A-10-AW, EKSPLA). The PL emission from samples was collected through a monochromator (SP2150, Princeton Instruments) equipped with a photomultiplier tube (PMT) (Hamamatsu, H10721-20) and the output signal from the PMT was recorded with a digital oscilloscope (DSO-X 3054A, Agilent). Decay profiles of TRPL were fitted to multi-exponential decay functions of time and their average lifetimes were calculated. Transient photocurrent decay profiles of the perovskite solar cells (under the illumination of 0.027 sun) were recorded by a digital oscilloscope (DSO-X 3054A, Agilent) with 50Ω input termination (1 MΩ termination for photovoltage decay

measurement of the devices) and the 532 nm excitation (pulse energy attenuated to  $\sim 1 \mu\text{J}$ ) of an OPO laser system (NT 342A-10-AW, EKSPLA). Decay profiles were fitted to multi-exponential decay functions of time. Internal quantum efficiency (IQE) and external quantum efficiency (EQE) were measured by using quantum efficiency measurement system (Oriel Quantx-300, Newport) in range from 380nm to 880nm. The  $J-V$  curves were measured using a solar simulator (Newport, Oriel Sol2A Class ABA 94042A for unit cell and 94082A for mini module, respectively) with a source meter (Keithley 2420) at  $100 \text{ mWcm}^{-2}$ , AM 1.5 G illumination, and a calibrated Si-reference cell certified by the NREL. The environmental conditions for photovoltaic device test were maintained at a temperature of  $25 \text{ }^\circ\text{C}$  and a relative humidity of 25% RH. The temperature of the devices was maintained between  $30$  and  $40 \text{ }^\circ\text{C}$  by air cooling. The  $J-V$  curves of unit cells were measured along the reverse scan direction from  $1.5 \text{ V}$  to  $-0.2 \text{ V}$  or the forward scan direction from  $-0.2 \text{ V}$  to  $1.5 \text{ V}$ . The step voltage and scan speed were fixed at  $10 \text{ mV}$  and  $150 \text{ mV s}^{-1}$ , respectively. The  $J-V$  curves of mini modules were measured along the reverse scan direction from  $17 \text{ V}$  to  $-0.2 \text{ V}$  or the forward scan direction from  $-0.2 \text{ V}$  to  $17 \text{ V}$ . The step voltage and scan speed were fixed at  $10 \text{ mV}$  and  $150 \text{ mV s}^{-1}$ , respectively. For the mechanical stability test, mini module was tested by bending machine (F3-2S, Forehu) with  $10 \text{ mm}$  radius for 1000 cycle test. The test was conducted in two different direction. One was the top side (direction to gold electrode) and the other was the bottom side (direction to PEN substrate). All module performances were measured after every 250 cycles.

### Photostability test

The photostability test was measured by maximum power point tracking method with encapsulated devices. The devices were encapsulated using a getter-dispersed polymer-metal barrier films. The devices with  $\text{ITO/SnO}_2(\text{FAPbI}_3)_{0.95}(\text{MAPbBr}_3)_{0.05}/\text{Spiro-OMeTAD}/\text{Au}$  and

ITO/SnO<sub>2</sub>/ZSO/(FAPbI<sub>3</sub>)<sub>0.95</sub>(MAPbBr<sub>3</sub>)<sub>0.05</sub>/Spiro-OMeTAD/Au were kept under AM 1.5 G simulated sun light in nitrogen (N<sub>2</sub>) filled chamber. The device temperature in the chamber was maintained between 25 °C by cooling system. PCEs of devices were recorded for 120 hours using a source meter (Keithley 2420).

**Scheme S1.** Illustration of perovskite solar cell device structures and their characteristics at each deposition process.

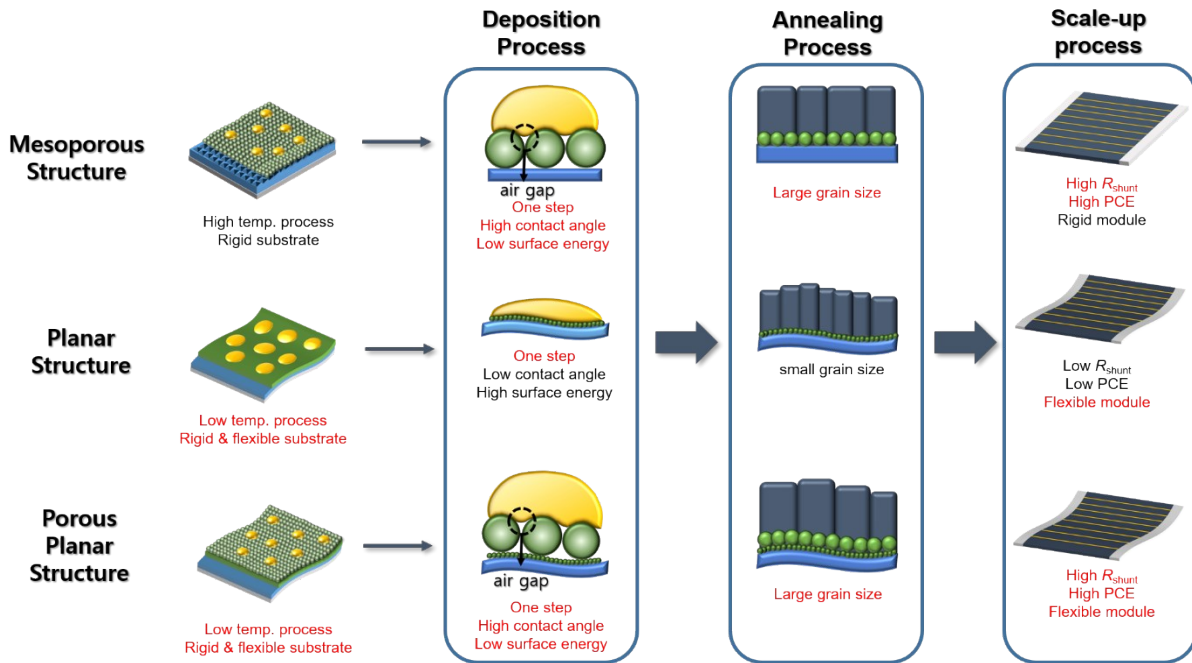


**Fig. S1.** SEM image of perovskite layer on ITO (a) and FTO substrate and AFM image of perovskite layer on ITO substrate (b) and (c) and on FTO substrate (d) and (e) .

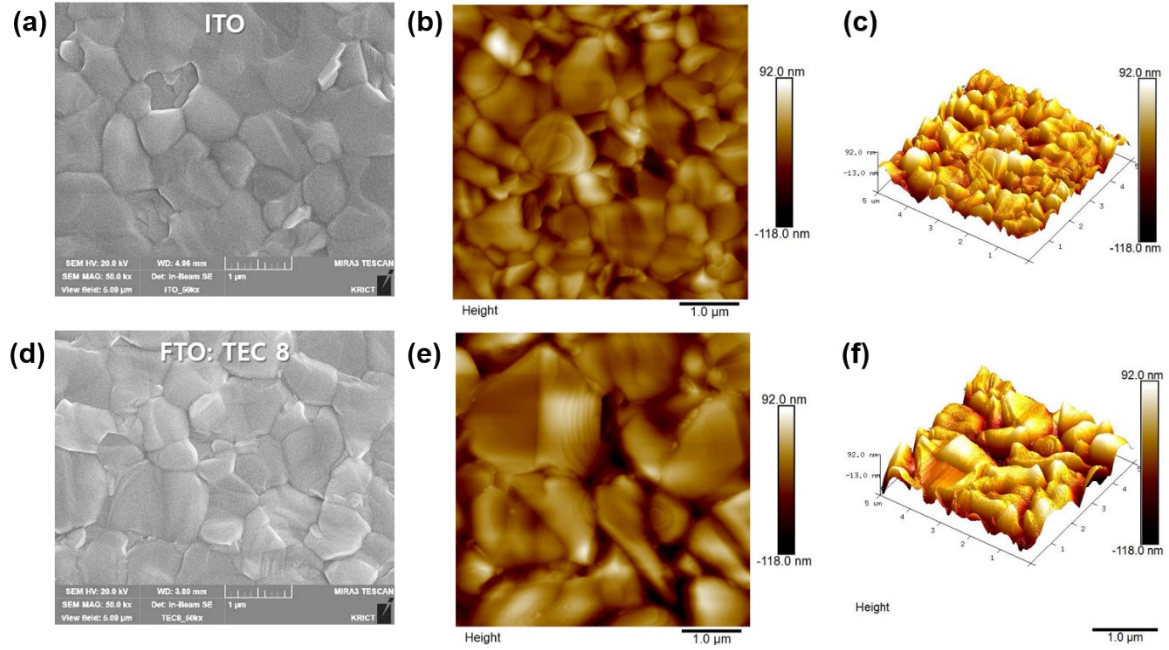


**Table 1.**  $R_q$  and  $R_a$  value of perovskite layer on each substrate

	<b>ITO</b>	<b>FTO: TEC 8</b>
$R_q$ (nm)	22.2	28.7
$R_a$ (nm)	17.1	22.1

**Fig. S2.** (a) Changing the particle size of metal oxide and (b) AFM image of their roughness according to particle size. (c) SEM image of corresponding perovskite layer.

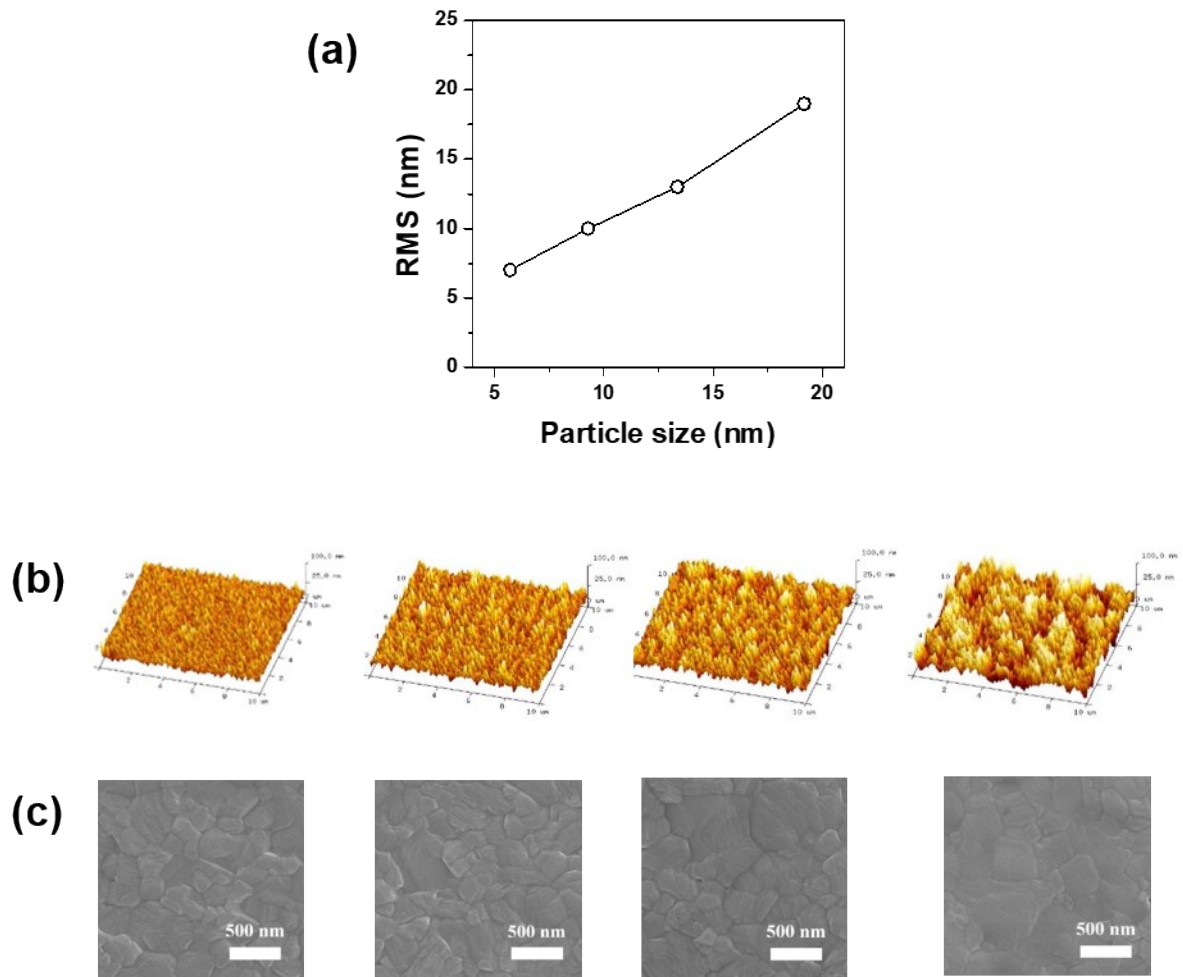


**Fig. S3.** (a) UPS total result, (b) UPS valence band maximum spectra, and (c) UPS cutoff edges of planar ( $\text{SnO}_2$ ) and porous planar ( $\text{Zn}_2\text{SnO}_4/\text{SnO}_2$ )

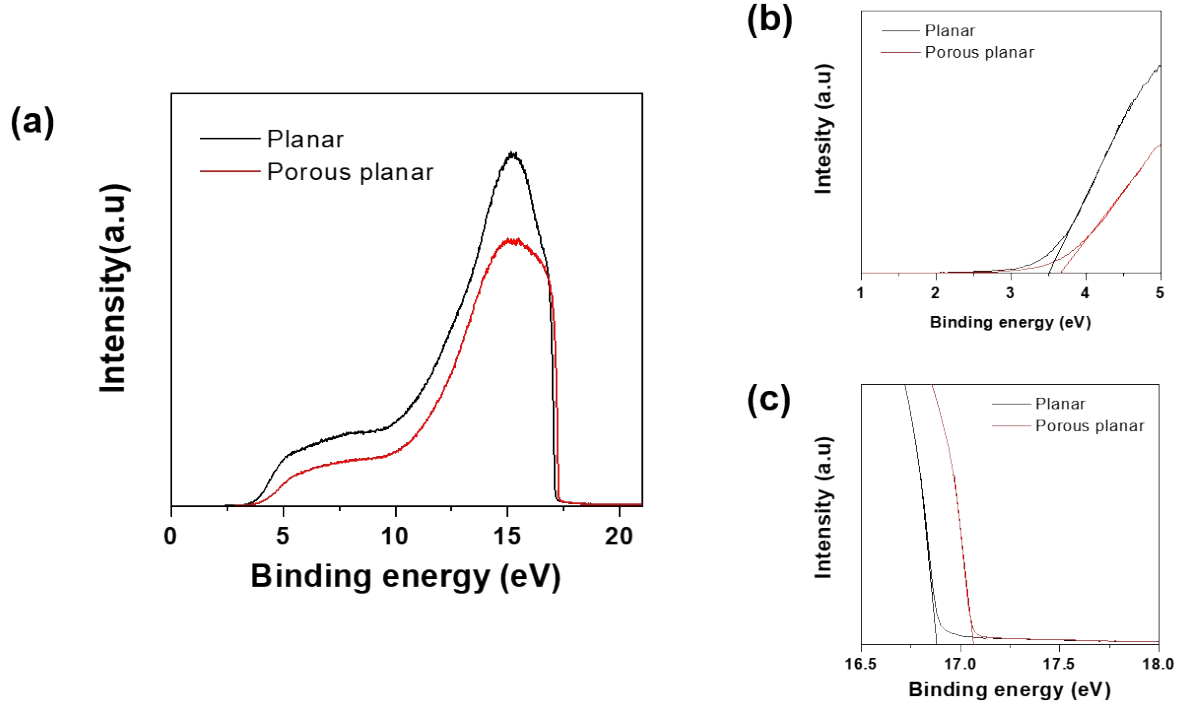


**Table S2.** Calculated work function, valence band, and conduction band position of each ETL

	$h\nu$	$E_{\text{cutoff}}$	$\Phi$	$E_{\text{vbm}}$	Valence band position	band gap	Conduction band position
<b>Planar</b>	21.2	16.89	4.31	3.5	7.81	3.57	4.24
<b>Porous planar</b>	21.2	17.06	4.14	3.64	7.78	3.65	4.13

**Fig. S4.** STEM-BF image of (A) planar ( $\text{SnO}_2$ ) layer and (B) porous planar ( $\text{Zn}_2\text{SnO}_4/\text{SnO}_2$ ) layer on ITO/glass substrate.

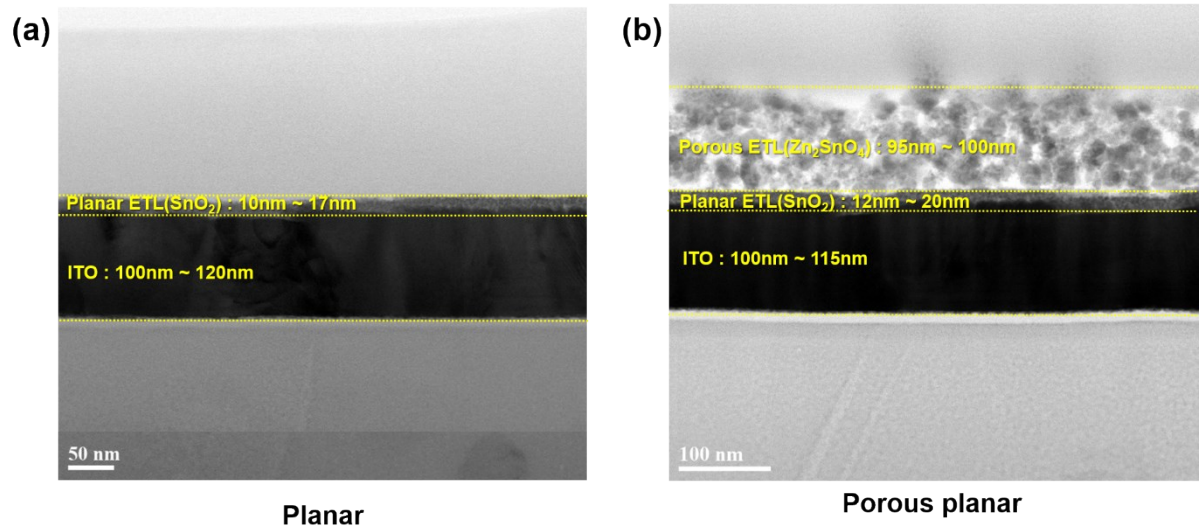


**Fig. S5.** (a) Best PCE and (b) steady state current of porous planar ( $\text{Zn}_2\text{SnO}_4/\text{SnO}_2$ ) PSC on glass substrate

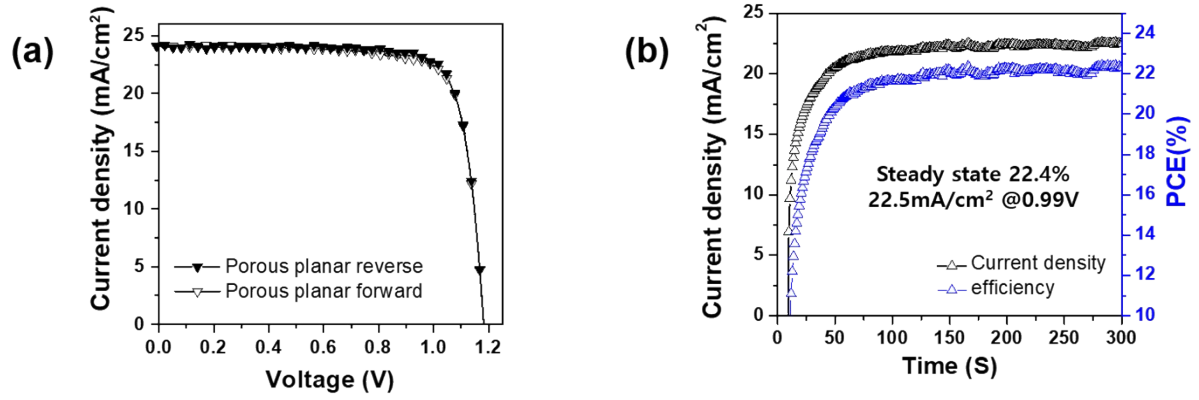


**Table S3.** Solar cell parameters for best PCE of porous planar ( $\text{Zn}_2\text{SnO}_4/\text{SnO}_2$ ) PSC on glass substrate.

	$V_{oc}$ (V)	$J_{sc}$ (mA/cm <sup>2</sup> )	FF (%)	Efficiency (%)
Porous planar on glass reverse	1.18	24.4	81.2	23.3
Porous planar on glass forward	1.18	24.5	79.2	22.9

**Fig. S6.** Histograms of the planar (black) and porous planar (red) based solar cell PCEs for 40 cells for (a)  $V_{OC}$ , (b)  $J_{SC}$ , (c) FF, and (d) efficiency.

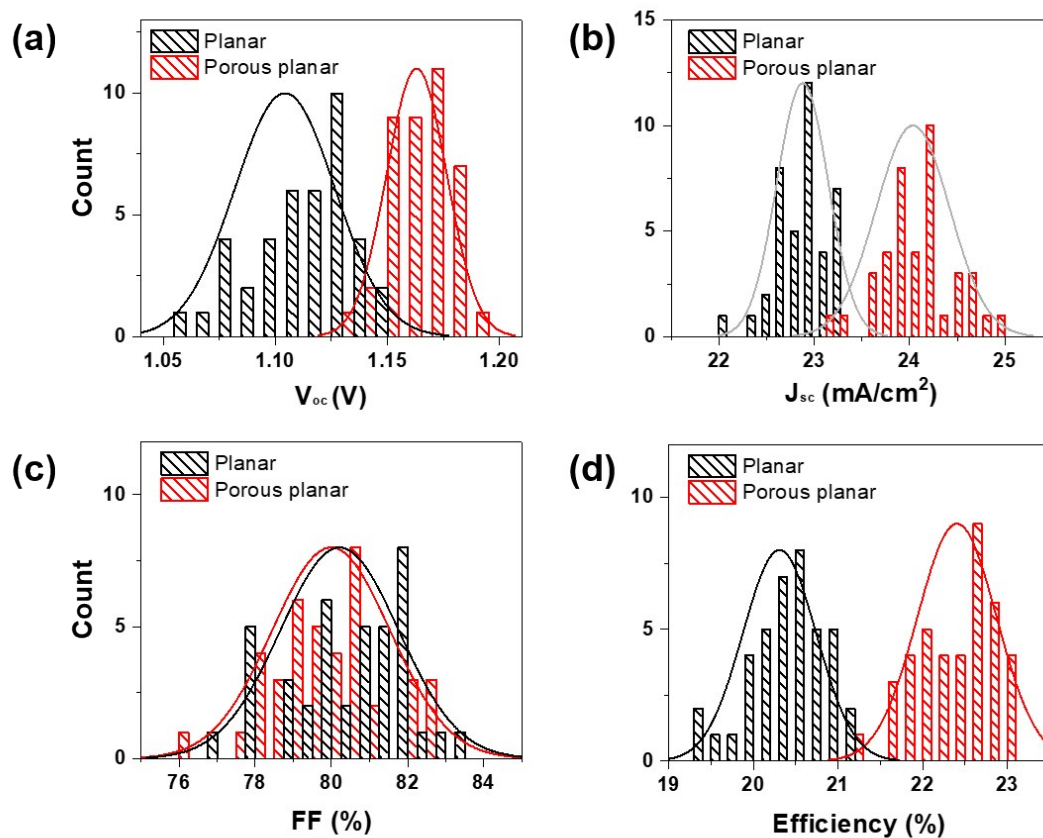


**Table S4.** The parameters of the porous planar (Zn<sub>2</sub>SnO<sub>4</sub>/SnO<sub>2</sub>) based perovskite solar cells.

	$V_{OC}$ (V)	$J_{SC}$ (mA/cm <sup>2</sup> )	FF (%)	Efficiency (%)
1	1.17	23.7	80.0	22.3
2	1.18	24.2	79.6	22.7
3	1.15	24.8	80.9	23.0
4	1.15	24.1	80.6	22.3
5	1.14	24.1	80.8	22.1
6	1.14	23.8	82.8	22.7
7	1.13	23.9	82.6	22.4
8	1.16	24.6	80.0	23.0
9	1.16	23.9	82.4	22.8
10	1.15	23.6	82.4	22.6
11	1.15	24.5	81.4	23.1
12	1.17	23.8	79.0	21.9
13	1.17	23.3	78.6	21.6
14	1.16	24.0	76.0	21.2
15	1.18	23.9	79.5	22.5
16	1.19	24.4	78.0	22.6
17	1.18	24.3	79.8	22.9
18	1.17	24.2	80.7	22.8
19	1.16	23.8	80.6	22.4
20	1.18	24.5	79.3	23.1
21	1.17	24.2	80.5	22.9
22	1.18	24.0	79.9	22.6
23	1.18	24.2	78.0	22.5
24	1.17	24.0	79.5	22.3
25	1.17	24.1	77.7	21.8
26	1.16	24.1	80.6	22.7
27	1.15	24.9	80.1	22.9
28	1.15	24.6	80.2	22.7
29	1.15	23.9	79.0	21.9
30	1.17	23.7	79.1	21.9
31	1.16	23.9	79.3	22.1
32	1.18	24.6	78.4	22.7
33	1.17	24.1	78.6	22.1
34	1.17	23.5	78.4	21.7
35	1.15	23.7	79.1	21.6
36	1.16	24.1	78.7	22.0
37	1.17	23.7	82.4	22.8
38	1.16	23.1	82.9	22.1
39	1.15	23.6	81.3	22.2
40	1.16	24.0	80.9	22.7
<b>Average</b>	<b>1.16</b>	<b>24.0</b>	<b>80.0</b>	<b>22.4</b>

**Table S5.** The parameters of the planar (SnO<sub>2</sub>) based perovskite solar cells.

	$V_{OC}$ (V)	$J_{SC}$ (mA/cm <sup>2</sup> )	FF (%)	Efficiency (%)
1	1.07	22.8	80.8	19.8
2	1.09	23.3	81.4	20.8
3	1.08	23.3	81.9	20.6
4	1.08	22.4	81.6	19.7
5	1.10	22.6	82.2	20.6
6	1.10	23.0	81.1	20.5
7	1.09	22.6	83.2	20.5
8	1.06	22.7	80.5	19.5
9	1.09	22.5	81.0	19.9
10	1.09	22.6	79.7	19.8
11	1.07	22.8	82.5	20.2
12	1.11	22.6	81.3	20.5
13	1.11	22.9	80.3	20.6
14	1.07	22.9	81.7	20.1
15	1.12	23.3	79.6	20.7
16	1.11	22.9	81.7	20.8
17	1.07	22.7	81.5	19.9
18	1.05	22.5	81.2	19.3
19	1.11	22.9	81.7	20.8
20	1.10	22.9	80.2	20.1
21	1.10	22.7	80.5	20.0
22	1.12	22.8	81.6	20.8
23	1.13	23.3	79.7	21.0
24	1.13	23.1	78.7	20.7
25	1.12	23.2	77.9	20.4
26	1.12	23.0	79.2	20.5
27	1.12	22.9	78.9	20.4
28	1.11	23.1	79.7	20.4
29	1.12	22.7	78.7	20.1
30	1.10	23.2	79.8	20.3
31	1.11	22.9	79.5	20.2
32	1.14	22.8	80.6	20.9
33	1.12	23.1	77.7	20.3
34	1.10	23.0	76.5	19.3
35	1.14	22.9	80.5	21.0
36	1.13	23.0	79.1	20.5
37	1.12	23.2	77.5	20.3
38	1.12	23.1	77.9	20.3
39	1.12	22.8	77.9	20.0
40	1.13	22.1	81.5	20.3
<b>Average</b>	<b>1.10</b>	<b>22.9</b>	<b>80.2</b>	<b>20.3</b>

**Fig. S7.** Photostability of planar and porous planar device measured by maximum power point tracking method for 120 hours.

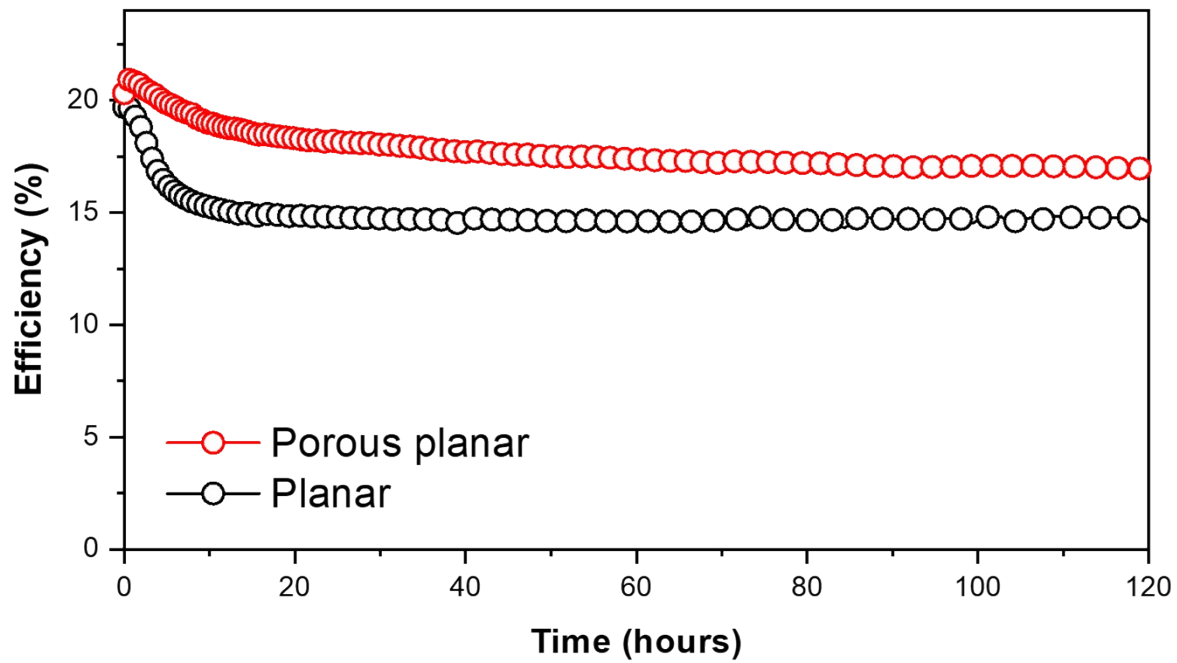


**Fig. S8.** SEM image of perovskite layer on (a) planar ( $\text{SnO}_2$ ) and (b) porous planar ( $\text{Zn}_2\text{SnO}_4/\text{SnO}_2$ ) ETL and (c) and (d) their grain size distribution.

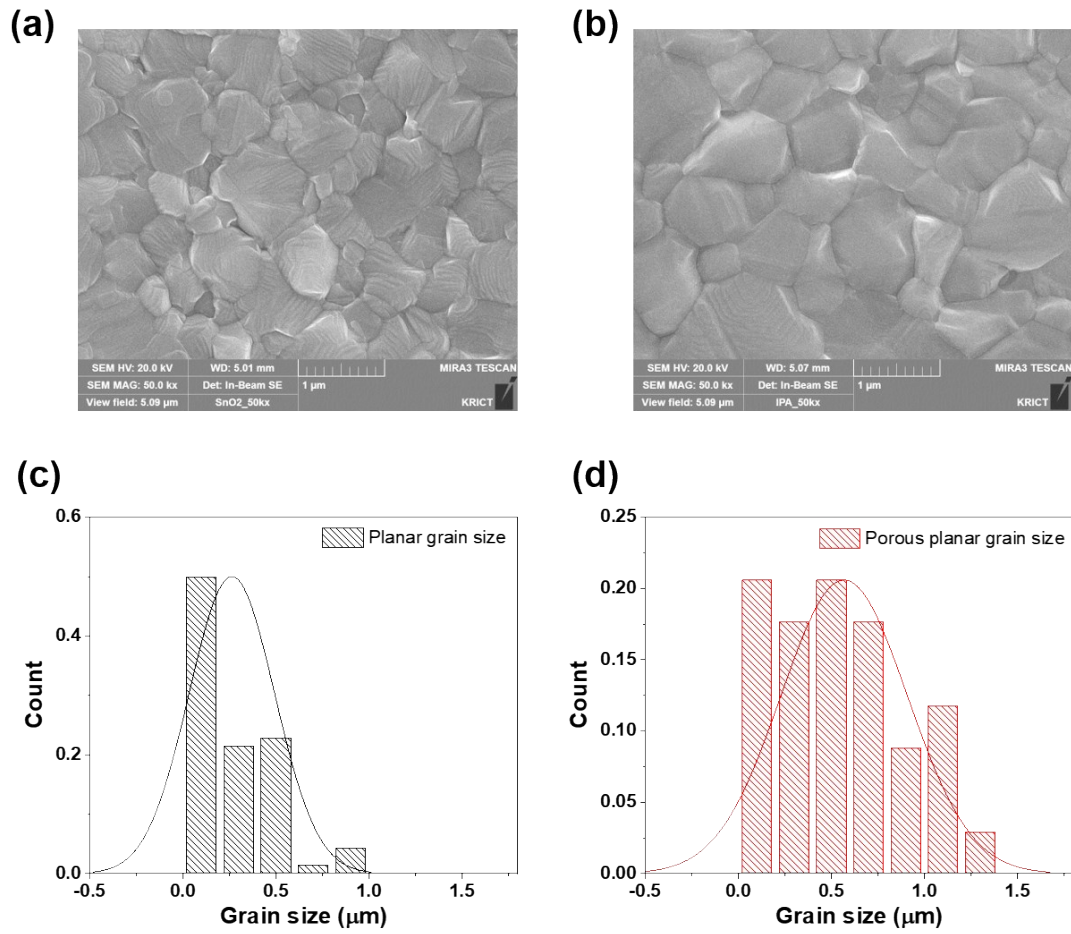


**Table. S6.** Average, maximum, and minimum grain size of perovskite on planar ( $\text{SnO}_2$ ) and porous planar ( $\text{Zn}_2\text{SnO}_4/\text{SnO}_2$ ) ETL.

grain size	Average ( $\mu\text{m}$ )	Max. ( $\mu\text{m}$ )	Min. ( $\mu\text{m}$ )
Porous planar $\text{Zn}_2\text{SnO}_4$	0.57	1.25	0.13
Planar $\text{SnO}_2$	0.26	0.97	0.14

**Fig. S9.** Contact angle of water on (a) planar ( $\text{SnO}_2$ ) and (b) porous planar ( $\text{Zn}_2\text{SnO}_4/\text{SnO}_2$ ) ETL.

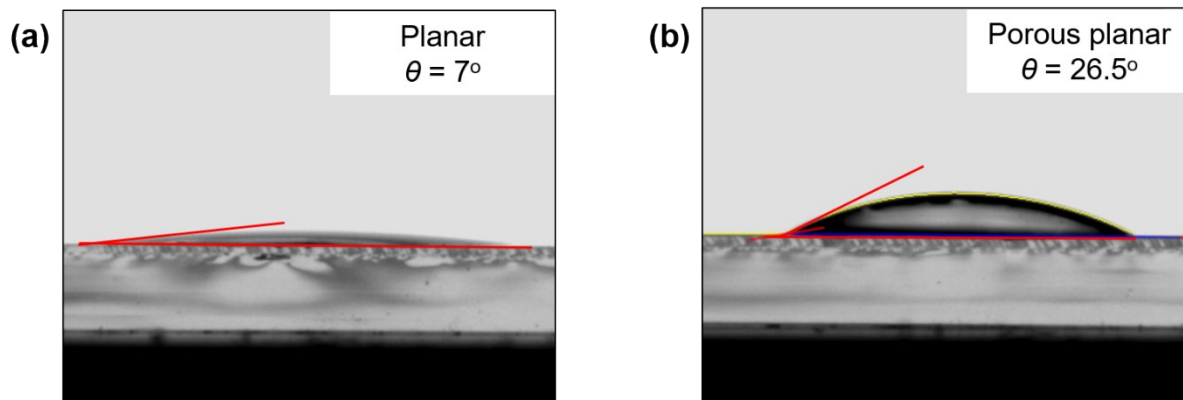


Fig. S10. (a) XPS spectra and (b) deconvolution results of SnO<sub>2</sub> and Zn<sub>2</sub>SnO<sub>4</sub>

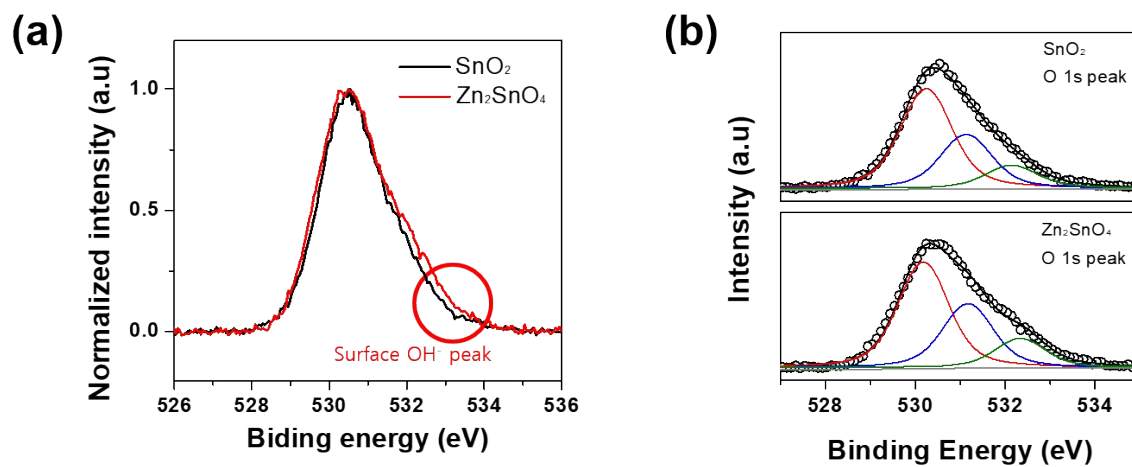
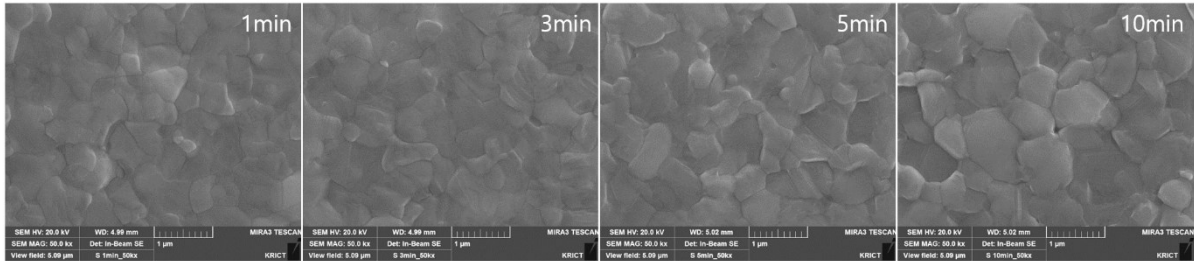


Table. S7. XPS deconvolution results of SnO<sub>2</sub> and Zn<sub>2</sub>SnO<sub>4</sub>

	O <sup>4-</sup>	O <sup>2-</sup>	O <sub>abs</sub>
SnO <sub>2</sub>	55.9 %	30.3 %	13.8 %
Zn <sub>2</sub> SnO <sub>4</sub>	53.1 %	32.2 %	14.7 %

**Fig. S11.** SEM image of perovskite layer annealing at 100 °C for 1 to 10 min on (a) planar ( $\text{SnO}_2$ ) and (b) porous planar ( $\text{Zn}_2\text{SnO}_4/\text{SnO}_2$ ) ETL.

(a)



(b)

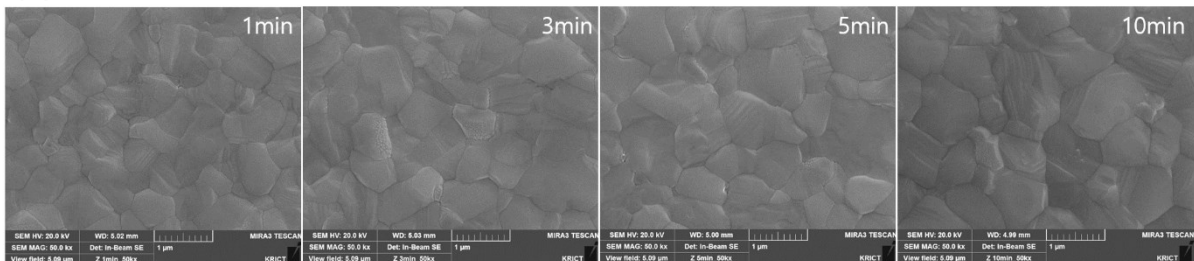


**Fig. S12.** Certification result of porous planar ( $Zn_2SnO_4/SnO_2$ ) based PSC on flexible PEN substrate tested at an independent and accredited PV testing lab (Newport).

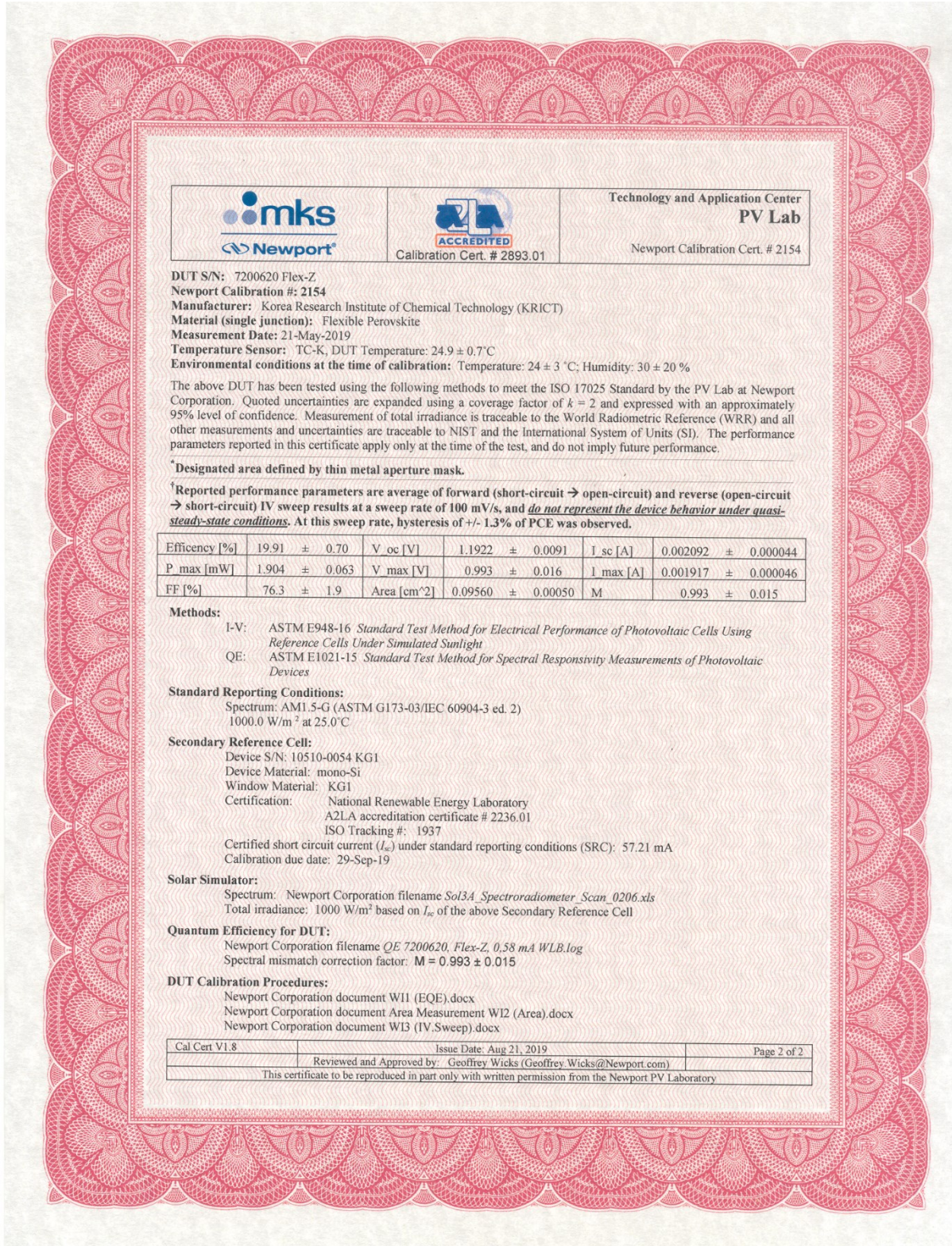


**Table S8.** Device performance of the state of art of flexible perovskite solar cells.

	Structure	$J_{SC}$	$V_{OC}$	FF	Eff.	year	Ref.
1	PEN/ITO/ZnO/MAPbI <sub>3</sub> /PTAA/Au	18.7	1.1	76	15.60%	2016	J. Mater. Chem. A, <b>4</b> , 1572-1578
2	PEN/ITO/ED-TiO <sub>2</sub> /BK-TiO <sub>2</sub> /MAPbI <sub>3</sub> /spiro-OMeTAD/Au	19.51	1.07	75	15.76%	2017	Adv. Energy. Mater., <b>7</b> , 1700169
3	PET/ITO/CPTA/MAPbI <sub>3</sub> /spiro-OMeTAD/Au	21.35	1.09	73.1	17.04%	2017	Adv. Energy. Mater., <b>7</b> , 1701144
4	PET/ITO/SnO <sub>2</sub> /C60-SAM/MA <sub>1-x</sub> FA <sub>x</sub> PbI <sub>3</sub> /Spiro-OMeTAD/Au	22.2	1.08	75.1	17.96%	2017	Nano Energy
5	PET/ITO/treated SnO <sub>2</sub> /C60-SAM/MA <sub>1-x</sub> FA <sub>x</sub> PbI <sub>3</sub> /Spiro-OMeTAD/Au	22.1	1.1	75.4	18.36%	2017	ACS Energy Lett., <b>2</b> , 2118-2124
6	PEN/ITO/C60/MAPbI <sub>3</sub> /spiro-OMeTAD/Au	18.1	1.01	70	13.90%	2018	Sci. Rep., <b>8</b> , 442
7	PEN/ITO/SnO <sub>2</sub> QDs/Cs <sub>0.05</sub> (MA <sub>0.17</sub> FA <sub>0.83</sub> ) <sub>0.95</sub> Pb(I <sub>0.83</sub> Br <sub>0.17</sub> ) <sub>3</sub>	20.94	1.11	0.73	16.97%	2018	Adv. Mater., <b>30</b> , 1706023
8	PEN/ITO/SnO <sub>2</sub> /Cs <sub>0.05</sub> (MA <sub>0.17</sub> FA <sub>0.83</sub> ) <sub>0.95</sub> Pb(I <sub>0.83</sub> Br <sub>0.17</sub> ) <sub>3</sub> /spiro-OMeTAD/Au	20	1.16	73.1	17.7%	2018	J. Phy. Chem. Lett., <b>9</b> , 5460-5467
9	PEN/ITO/Ti-MOF/PCBM/(MAPbI <sub>3</sub> ) <sub>0.95</sub> (FAPbI <sub>3</sub> ) <sub>0.05</sub> /spiro-OMeTAD/Au	22.6	1.05	73.4	17.43%	2018	Acs Nano, <b>12</b> , 4968-4975
10	PET/ITO/SnO <sub>2</sub> /Al <sub>2</sub> O <sub>3</sub> /Cs <sub>0.05</sub> (FA <sub>0.83</sub> MA <sub>0.17</sub> ) <sub>0.95</sub> PbI <sub>2.5</sub> Br <sub>0.5</sub> /spiro-OMeTAD/Au	22.8	1.05	76	18.10%	2018	ACS Energy Lett., <b>3</b> , 1482-1491
11	PET/ITO/E-SnO <sub>2</sub> /FA <sub>0.95</sub> Cs <sub>0.05</sub> I <sub>3</sub> /spiro-OMeTAD/Au	23.42	1.09	71.6	18.28%	2018	Nature. Comm., <b>9</b> , 3239
12	PET/ITO/Nb <sub>2</sub> O <sub>5</sub> /MAPbI <sub>3</sub> -DS/Spiro-OMeTAD/Au	22.48	1.1	74.2	18.4%	2018	Adv. Mater., <b>30</b> , 1801418
13	PET/ITO/SnO <sub>2</sub> /FAMAPbI <sub>3</sub> /Spiro-OMeTAD/Au	22.48	1.11	68.49	17.09%	2019	ACS Sustainable Chem. Eng., <b>7</b> , 4343-4350
14	PEN/ITO/SnO <sub>2</sub> /Cs <sub>0.05</sub> (FA <sub>0.85</sub> MA <sub>0.15</sub> ) <sub>0.95</sub> Pb(I <sub>0.85</sub> Br <sub>0.15</sub> ) <sub>3</sub> /Spiro-OMeTAD/Au	20.3	1.15	75	17.50%	2019	Adv. Energy. Mater., <b>9</b> , 1900834
15	PEN/ITO/graphene-SnO <sub>2</sub> /CsFAMAPbI <sub>3</sub> /Spiro-OMeTAD/Au	22.1	1.07	75	17.70%	2019	J. Mater. Chem. A, <b>5</b> , 13639-13647
16	PEN/ITO/SnO <sub>2</sub> /MAPbI <sub>3</sub> /Spiro-OMeTAD/Ag	21.8	1.13	72.78	18.00%	2019	Adv. Funct. Mater., <b>29</b> , 1900557
17	PEN/ITO/CPTA/SnO <sub>2</sub> /C60/Cs <sub>0.05</sub> FA <sub>0.81</sub> MA <sub>0.14</sub> PbI <sub>2.55</sub> Br <sub>0.45</sub> /spiro-OMeTAD/Au	21.35	1.11	76.6	18.10%	2019	Adv. Funct. Mater., <b>29</b> , 1807604
18	PET/ITO/SnO <sub>2</sub> /KCl/MAPbI <sub>3</sub> /spiro-OMeTAD/Ag	20.69	1.11	81	18.53%	2019	ACS appl. Energy Mater., <b>2</b> , 3676-3682
19	PEN/ITO/HfO <sub>2</sub> /SnO <sub>2</sub> /(Rb <sub>1</sub> K <sub>4</sub> CsFAMA)PbI <sub>3</sub> /Spiro-OMeTAD/Au	21.24	1.135	73.2	19.11%	2019	J. Mater. Chem. A, <b>7</b> , 4960-4970
20	Willow Glass/ITO/PTAA/MAPbI <sub>3</sub> /C60/BCP/Cu	21.49	1.09	79.1	19.72%	2020	Adv. Energy. Mater., <b>10</b> , 1903108
21	PEN/ITO/NiO <sub>x</sub> /FA <sub>1-x</sub> MA <sub>x</sub> PbI <sub>y</sub> Br <sub>3-y</sub> /Spiro-OMeTAD/Au	22.2	1.12	74	18.5	2020	Nano Energy, <b>70</b> , 104505
22	PEN/ITO/SnO <sub>2</sub> /ZSO/(FAPbI <sub>3</sub> ) <sub>0.95</sub> (MAPbI <sub>3</sub> ) <sub>0.05</sub> /spiro-OMeTAD/Au	21.9	1.19	79.6	20.75%	2020	this work

**Fig. S13.** Histograms of the porous planar ( $\text{Zn}_2\text{SnO}_4/\text{SnO}_2$ ) based flexible perovskite solar cell PCEs for 22 cells

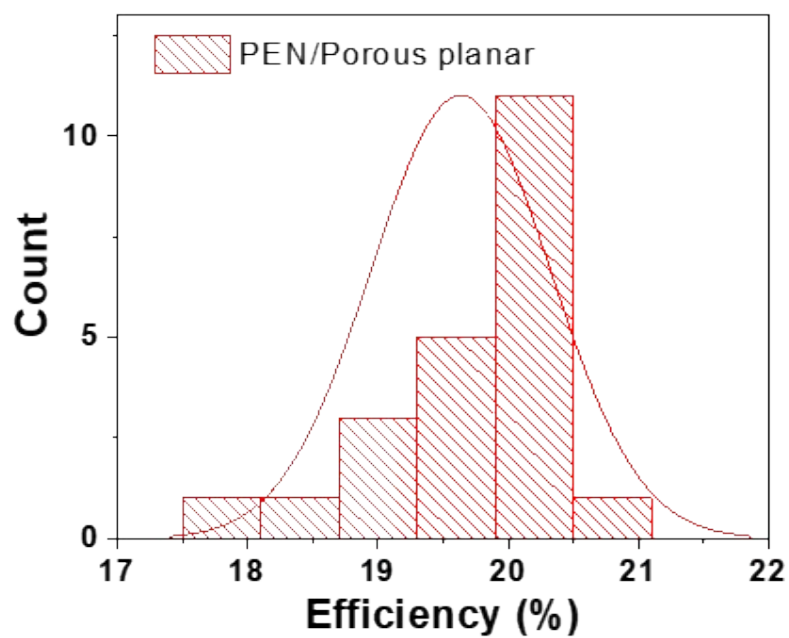


**Table S9.** The parameters of the porous planar (Zn<sub>2</sub>SnO<sub>4</sub>/SnO<sub>2</sub>) based flexible perovskite solar cells.

	<i>V<sub>oc</sub></i> (V)	<i>J<sub>sc</sub></i> (mA/cm <sup>2</sup> )	FF (%)	Efficiency (%)
1	1.12	21.8	76.2	18.7
2	1.12	22.1	78.3	19.3
3	1.1	21.9	73.9	17.8
4	1.14	22	78.1	19.5
5	1.13	22.1	78	19.4
6	1.08	22.2	77.6	18.5
7	1.13	21.9	78.3	19.6
8	1.18	21.9	77.9	20.2
9	1.17	21.9	74.3	19.1
10	1.18	22.0	76.4	19.9
11	1.19	21.8	78.4	20.4
12	1.19	21.9	77.7	20.3
13	1.18	21.4	78.8	19.9
14	1.19	21.6	80.4	20.7
15	1.19	21.4	78.3	20.0
16	1.19	21.6	77.4	19.9
17	1.13	22	77.5	19.4
18	1.16	22.5	78.4	20.4
19	1.14	22.5	77.6	19.9
20	1.14	22.4	78.5	20
21	1.14	22.4	78.4	19.9
22	1.13	22.2	76.9	19.2
<b>Average</b>	<b>1.15</b>	<b>22.0</b>	<b>77.6</b>	<b>19.6</b>

Fig. S14. Dark J-V of planar and porous planar module (aperture area: 100cm<sup>2</sup>)

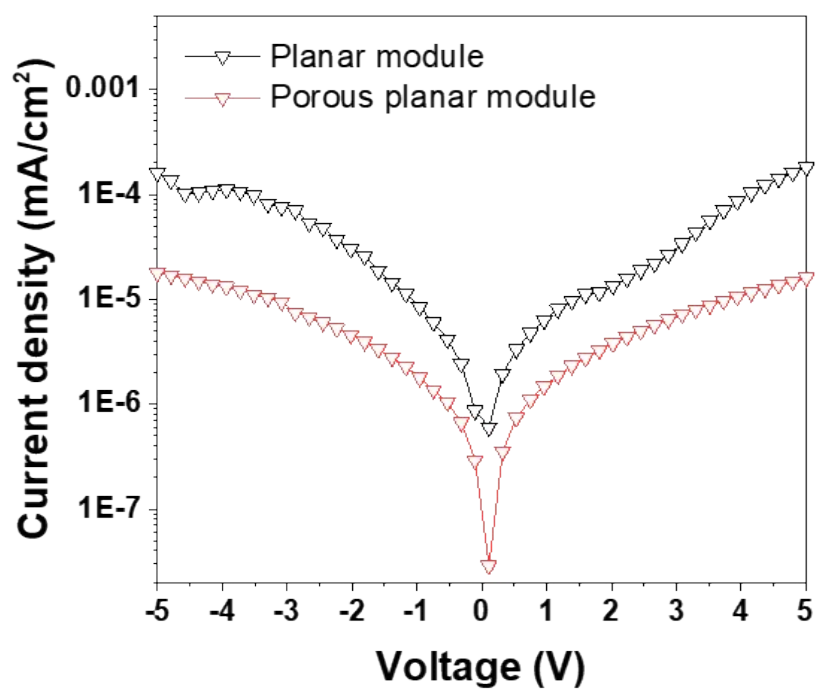


**Fig. S15.** Photograph of porous planar ( $\text{Zn}_2\text{SnO}_4/\text{SnO}_2$ ) based flexible sub-module with aperture area of unit cell ( $0.1 \text{ cm}^2$ ,  $100 \text{ cm}^2$ ,  $225 \text{ cm}^2$  and  $400 \text{ cm}^2$ ).

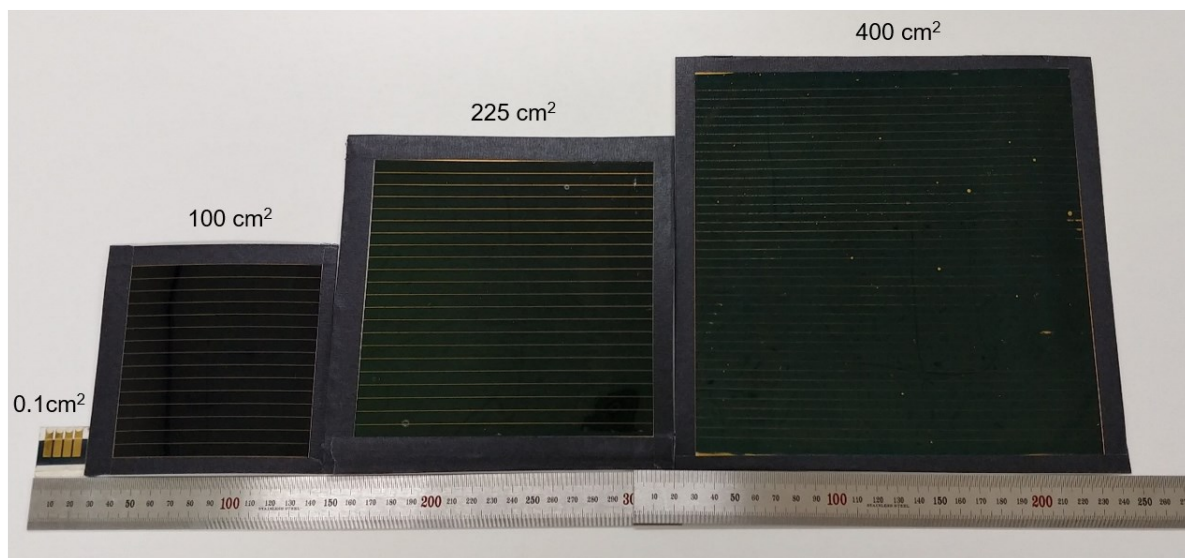


**Fig. S16.** Best PCE of porous planar ( $\text{Zn}_2\text{SnO}_4/\text{SnO}_2$ ) based flexible perovskite sub-module according to aperture (red) and active area (black).

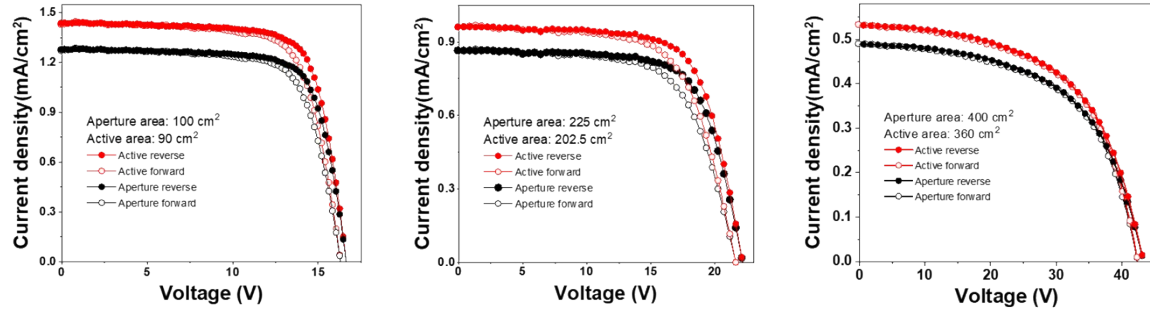


**Table S10.** PCE parameters of porous planar ( $\text{Zn}_2\text{SnO}_4/\text{SnO}_2$ ) based flexible perovskite sub-module according to aperture and active area.

		$V_{oc}$ (V)	$J_{sc}$ (mA/cm <sup>2</sup> )	FF (%)	Efficiency (%)
<b>Aperture size:</b> <b>100 cm<sup>2</sup></b>	Reverse	16.6	1.28	74.83	15.9
	Forward	16.3	1.27	72.59	15.0
<b>Active size:</b> <b>90 cm<sup>2</sup></b>	Reverse	16.6	1.44	74.83	17.9
	Forward	16.3	1.43	72.59	17.0

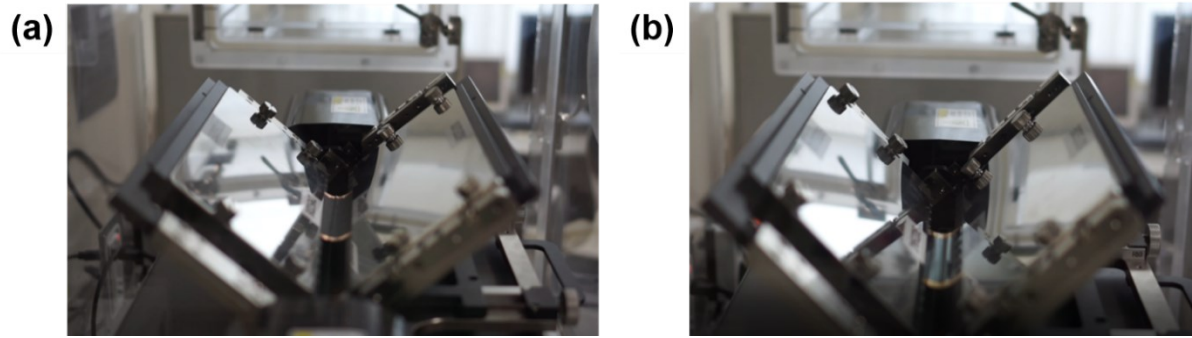
  

		$V_{oc}$ (V)	$J_{sc}$ (mA/cm <sup>2</sup> )	FF (%)	Efficiency (%)
<b>Aperture size:</b> <b>225 cm<sup>2</sup></b>	Reverse	22.1	0.87	70.0	13.4
	Forward	21.6	0.87	65.7	12.3
<b>Active size:</b> <b>202.5 cm<sup>2</sup></b>	Reverse	22.1	0.97	70.0	14.9
	Forward	21.6	0.97	65.7	13.7

		$V_{oc}$ (V)	$J_{sc}$ (mA/cm <sup>2</sup> )	FF (%)	Efficiency (%)
<b>Aperture size:</b> <b>400 cm<sup>2</sup></b>	Reverse	43.4	0.49	55.9	11.8
	Forward	42.3	0.49	56.8	11.8
<b>Active size:</b> <b>360 cm<sup>2</sup></b>	Reverse	43.4	0.54	55.9	13.1
	Forward	42.3	0.54	56.8	13.0

**Fig. S17.** Image of bending test in each directions (a) bend in (b) bend out



- 1 Yoo, J. J. *et al.* An interface stabilized perovskite solar cell with high stabilized efficiency and low voltage loss. *Energy & Environmental Science* **12**, 2192-2199, doi:10.1039/C9EE00751B (2019).